ARTICLE

Immobilizing Enzymes onto Electrode Arrays by Hydrogel Photolithography to Fabricate Multi-Analyte Electrochemical Biosensors

Jun Yan,[†] Valber A. Pedrosa,[‡] Aleksandr L. Simonian,[‡] and Alexander Revzin*[,†]

Department of Biomedical Engineering, University of California, Davis, 451 East Health Sciences Street, #2619, Davis, California 95616, and Department of Materials Engineering, Auburn University, Auburn, Alabama 36849

ABSTRACT This paper describes a biomaterial microfabrication approach for interfacing functional biomolecules (enzymes) with electrode arrays. Poly (ethylene glycol) (PEG) hydrogel photopatterning was employed to integrate gold electrode arrays with the enzymes glucose oxidase (GOX) and lactate oxidase (LOX). In this process, PEG diacrylate (DA)-based prepolymer containing enzyme molecules as well as redox species (vinylferrocene) was spin-coated, registered, and UV cross-linked on top of an array of gold electrodes. As a result, enzyme-carrying circular hydrogel structures (600 μm diameter) were fabricated on top of 300 μm diameter gold electrodes. Importantly, when used with multiple masks, hydrogel photolithography allowed us to immobilize GOX and LOX molecules on adjacent electrodes within the same electrode array. Cyclic voltammetry and amperometry were used to characterize biosensor electrode arrays. The response of the biosensor array was linear for up to 20 mM glucose with sensitivity of 0.9 μA cm^{-2} mM^{-1} and 10 mM lactate with sensitivity of 1.1 μA cm^{-2} mM^{-1}. Importantly, simultaneous detection of glucose and lactate from the same electrode array was demonstrated. A novel strategy for integrating biological and electrical components of a biosensor described in this paper provides the flexibility to spatially resolve and register different biorecognition elements with individual members of a miniature electrode array. Of particular interest to us are future applications of these miniature electrodes for real-time monitoring of metabolite fluxes in the vicinity of living cells.

KEYWORDS: hydrogel micropatterning • enzyme-based electrodes • microfabrication • glucose and lactate detection

INTRODUCTION

Enzyme-based electrodes represent an important class of biosensors where byproducts of enzymatic breakdown of an analyte are detected electrochemically (1−5). Of particular relevance are enzyme-based electrodes for detection of glucose and lactate, energy metabolites that are monitored closely in such diseases as diabetes, obesity and cancer (6−8). Recent emphasis in the development of electrochemical biosensors has been placed on multianalyte detection and miniaturization (9−13). The push for miniaturization has been aided by adaption of semiconductor fabrication processes for making and packaging of miniature electrodes (9, 14−18). However, immobilizing distinct biorecognition elements (e.g., enzymes) on different members of an electrode array, a requirement for multianalyte detection, remains challenging. The enzyme molecules are traditionally immobilized on electrodes using chemical cross-linking (19), electrodeposition (20, 21), electrostatic interactions (17, 22, 23), and membranes or carrier matrices (1, 2). These traditional strategies for enzyme immobilization are not well suited for depositing specific enzyme types onto a desired member of an electrode array.

Hydrogels are attractive materials in fabricating electrochemical biosensors because a hydrated gel provides an excellent matrix for encapsulation of functional enzymes (2, 4). A number of studies have used a uniform gel membrane coated on top of the microfabricated electrodes to prevent fouling and enzyme leaching (16, 24−27), whereas far fewer reports describe the integration of patterned gel layer with electrodes (10, 27, 28). The previous reports employed acrylamide, hydroxyl ethyl methacrylate (HEMA) or poly vinyl acetate (PVA) for hydrogel/electrode construction.

The goal of the present paper was to utilize poly(ethylene glycol) (PEG) hydrogel photolithography, a micropatterning process reported by us previously (29), in order to interface enzymes with microfabricated electrodes. PEG is a material of choice for preventing nonspecific binding and electrode fouling (4, 30) and has been used extensively for entrapment of functional enzymes (2, 29, 31−33). In this paper, we sought to leverage the excellent properties of this biomaterial in order to interface enzyme-carrying PEG hydrogels with Au electrodes. Our design criteria were (1) to demonstrate micropatterning of PEG hydrogel structures in registration with microfabricated Au electrodes, (2) to characterize function of glucose oxidase (GOX) and lactate oxidase (LOX) enzymes entrapped within hydrogel microstructures, (3) to develop redox hydrogels that circumvent the dependence of glucose and lactate sensors on diffusible species (e.g., oxygen), and (4) to place LOX- or GOX-carrying hydrogel microstructures on the adjacent electrodes of an electrode

* Corresponding author. E-mail: arevzin@ucdavis.edu.
Received for review November 10, 2009 and accepted February 2, 2010
[†] University of California.
[‡] Auburn University.
DOI: 10.1021/am9007819

Published on Web 02/16/2010

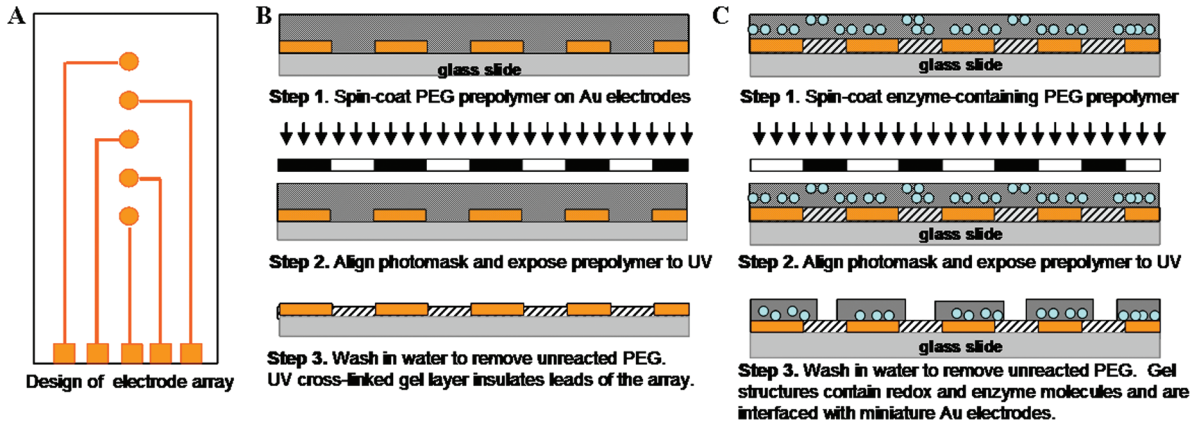

FIGURE 1. (A) Layout of an electrode array consisting of five 300 μm diameter Au electrodes, 15 μm wide leads, and 4 mm^2 contact pads. (B) Micropatterning PEG hydrogel to insulate the leads. This hydrogel layer does not have redox polymer or enzyme molecules. (C) Micropatterning enzyme-carrying hydrogel microstructures in alignment with microfabricated Au electrodes. This process can be repeated with multiple masks and different prepolymer formulations to immobilize distinct enzyme-carrying gel structures on different electrodes of the array.

array. The novel fabrication method and a microdevice described here represent an important step toward development of biosensors capable of interfacing with living cells for in vitro monitoring cell metabolite fluxes.

MATERIALS AND METHODS

Materials. Poly (ethylene glycol) diacrylate (PEG-DA, MW 575), 2-hydroxy-2methyl-propiophenone (photoinitiator), 99.9% toluene, (EC 1.1.3.4, type II—S from *Aspergillus niger* (18 000 U g^{-1} solid), $MgCl_2 \cdot 6H_2O$, D-(+)-glucose, vinylferrocene, and horseradish peroxidase (HRP) were purchased from Sigma (St Louis, MO. Amplex Red was purchased from Invitrogen (Carlsbad, CA). Lactate oxidase (E.C. 1.1.3.2 from Pediococcus sp) was obtained from MP biomedicals (Solon, OH). Phosphate buffer (PBS) 10 mM was used as a supporting electrolyte for all electrochemistry experiments. Chromium etchant (CR-4S) and gold etchant (Au-5) were from Cyantek Corporation (Fremont, CA). Positive photoresist (AZ 5214-E IR) and its developer solution (AZ300 MIF) were brought from Mays Chemical (Indianapolis, IN). 3-Acryloxypropyl trichlorosilane was from Gelest, Inc. (Morrisville, PA). Water used for preparation of aqueous solutions came from a Millipore Direct-Q water purification system (resistivity, 18 MΩ cm^{-2}). D-(+)-Glucose solutions were allowed to muta-rotate overnight at room temperature before use. Stock solutions were prepared in bidistilled water or PBS solution and stored in the dark at 4 °C.

Equipment. All voltammetric and amperometric experiments were performed using a CH Instruments (CH1910B) Bi-Potentiostat. All experiments were conducted in a three electrode system containing a platinum wire auxiliary electrode, a saturated Ag/AgCl (3 M) reference electrode and enzyme-modified working electrode. The buffer solution was 10 mM PBS with 20 μM $MgCl_2$. The buffer solution was deoxygenated with N_2 for 10 min before electrochemistry measurements. All electrochemical measurements were performed at room temperature.

Fabrication of Au Electrode Arrays. The layout of electrode array was designed in AutoCAD, converted into plastic transparencies by CAD Art Services (Portland, OR) and then transferred onto quartz/chrome plates using standard photolithography and wet etching approaches. The design of the Au electrode arrays is shown in Figure 1A.

To fabricate gold electrode arrays, we sputter-coated standard (75 mm × 25 mm) glass slides with 15 nm Cr adhesion layer and 100 nm Au layer by Lance Goddard Associates (Santa Clara, CA). The electrodes were fabricated using traditional photoresist lithography and wet etching processes. Importantly, the photoresist layer was not removed immediately after metal etching but was employed to protect underlying Au regions during the silane modification protocol described below. The etching of Au/chrome layers resulted in an array of five working microelectrodes patterned on a glass slide. Each Au electrode was 300 μm in diameter with 15 μm wide leads and 2 mm × 2 mm square contact pad (see Figure 1A for layout of electrodes). Wires were soldered to contact pads to connect electrode arrays to the potentiostat during electrochemistry experiments.

Integration of Au Electrodes with Enzyme-Carrying Hydrogel Microstructures. The glass substrates with photoresist-covered Au electrodes were modified using acrylatyed silane coupling agent following the protocol described by us previously (35). This step was necessary to ensure covalent anchoring of hydrogel structures onto the glass substrates. After the silane modification step, substrates were sonicated in acetone for 2 min to remove the photoresist and then placed in an oven for 3 h at 100 °C to cross-link the silane layer.

When preparing enzyme electrodes, GOX was dissolved in PBS buffer (pH 6.0) to reach the concentration of 20 mg/mL while LOX was dissolved in PBS buffer (pH 6.5) to concentration of 15 mg/mL. Glutaraldehyde was added to the enzyme solution at 2% v/v to improve enzyme retention and function of the biosensor. In parallel, the prepolymer solution was prepared by adding 2% (v/v) of photoinitiator (2-hydroxy-2-methyl-propiophenone) and 1% (v/v) of vinlyferrocene to PEG-diacrylate (DA) (MW 575). Enzyme and prepolymer solution were combined by adding 0.2 mL of the enzyme solution to 0.8 mL of PEG-DA/vinylferrocene. The mixture was stirred for 4 h at 4 °C to ensure the homogeneous dispersion of the enzyme molecules.

In the next step, PEG prepolymer solution containing enzyme molecules and redox species was photopolymerized on top of the Au electrodes in a process similar to photolithography (see Figure 1B,C). PEG-based prepolymer solution was spin-coated at 800 rpm for 4 s onto glass slides containing Au electrode patterns. A photomask was registered with an electrode pattern and then exposed to unfiltered UV light at 65 mW/cm^2 for 10 s to convert liquid prepolymer into cross-linked hydrogel. The surfaces were developed in DI water for 3 min to remove unpolymerized PEG precursor solution. Enzyme carrying hydrogel microstructures were made larger than Au electrodes, 600 and 300 μm diameter for hydrogel and Au features, respectively. This was done to ensure effective anchoring of the hydrogel structures to silanized glass substrate.

The spin—align—expose hydrogel patterning process described above was carried out three times in order to deposit three distinct, coplanar hydrogel layers onto the substrate. The first hydrogel layer contained no enzymes or redox species and

was deposited selectively onto the leads, leaving circular electrode and contact pad regions open (see Figure 1B). This step was needed to insulate nonsensing Au regions of the electrode array. In the next step, GOX- and redox species-carrying PEG prepolymer solution was spin-coated and photopolymerized in registration with the desired electrodes of the array. After this step, shown in Figure 1C, select members of the electrode array contained GOX-carrying hydrogel microstructures. In the final step of fabrication process, LOX-containing redox hydrogels were deposited onto remaining Au electrodes. This multistep process resulted in construction of an array of miniature Au electrodes with alternating electrodes carrying either glucose- or lactate-sensing enzymes.

To help visualize deposition of different types of hydrogel microstructures on adjacent electrodes, we utilized Amplex red-based fluorescence reporter system. Amplex red is a nonfluorescent molecule that is oxidized into a fluorescent compound during horseradish peroxidase (HRP)-catalyzed breakdown of H_2O_2. In this experiment, 100 μL of Amplex Red/HRP/PEG-DA precursor solution was prepared by mixing 5 μL of 50 mM Amplex Red stock solution with 5 μL of HRP (1 mg/mL) and 90 μL of PEG precursor solution. Amplex Red/HRP PEG precursor solution and pure PEG solution were deposited onto adjacent Au electrodes using a multistep patterning process described above. Hydrogel containing electrodes were immersed in PBS containing 5 mM of H_2O_2 and were observed using upright fluorescence microscope (Nikon Eclipse LV100).

Electrochemical Characterization of Enzyme Electrodes. Electrodes were tested in a custom-made, Plexiglas electrochemical cell with a volume of ~1 mL. PBS (pH 7.0) with 20 μM $MgCl_2$ was degassed with N_2 and served as electrolyte during experiments. Two electrochemistry techniques, cyclic voltammetry and amperometry, were used to characterize the sensor response to glucose and lactate. D-Glucose and lactic acid solutions were stored overnight at room temperature to allow equilibration of the α- and β- forms.

To characterize redox properties of vinylferrocene-containing hydrogel, we used cyclic voltammetry with scan rates ranging from 10 to 50 mV/s. When performing amperometry experiments, we poised the enzyme-containing working electrode at 0.4 V (vs Ag/AgCl) (anodic peak potential of immobilized vinylferrocene) and exposed it to aliquots of glucose or lactate. Analyte concentration in the electrochemical cell was adjusted in 1 to 2 mM increments. Analytes were added after the background current has stabilized. For sensor stability experiments, fabricated enzyme electrodes were stored at 4 °C in 1× PBS between tests.

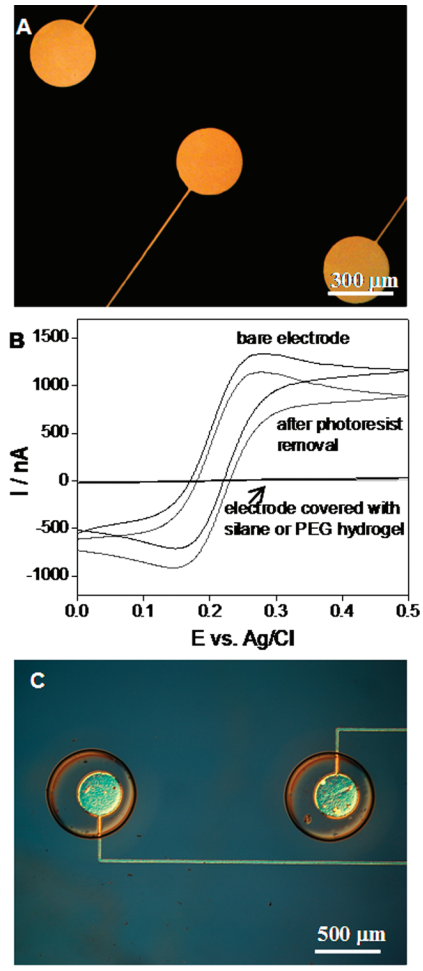

FIGURE 2. (A) Portion of five-electrode array with 300 μm diameter Au electrodes and 15 μm diameter leads. Contact pads are not shown in this image. (B) Cyclic voltammetry characterization of bare vs photoresist protected electrodes after silane modification. Ferricyanide was used as diffusible redox species to test the electron transfer. The scan rate was 20 mV/s Ag/AgCl reference and Pt counter electrodes were used. Electrodes modified with silane or coated with hydrogel were similarly resistive and CV curves for these two conditions overlap. Insulating PEG hydrogel coating did not contain redox polymer. (C) Hydrogel microstructures (600 μm diameter) fabricated on top of the 300 μm Au electrodes. The hydrogel structures were made larger than electrodes to ensure attachment of gel to the glass substrate modified with acrylated silane.

RESULTS AND DISCUSSION

In the present study, PEG hydrogel microfabrication was employed to integrate and package miniature Au electrodes with enzyme-carrying hydrogel structures. This novel fabrication approach allowed to deposit GOX- and LOX-carrying hydrogels on the adjacent members of an electrode array. Electrochemical testing was employed to characterize sensor response to glucose and lactate, and to demonstrate simultaneous response to both analytes from the same electrode array. The use of PEG hydrogel, a nonfouling and enzyme-friendly material, for construction of miniature enzyme electrodes opens future possibility for interfacing electrodes with living cells for dynamic monitoring of cell function.

Surface Modification and Fabrication of Electrodes. An array of individually addressable Au electrodes (layout shown in Figure 1) consisted of 300 μm diameter electrodes connected to contact pads via 15 μm wide leads. An image of three electrodes is shown in Figure 2A. Upon patterning of Au electrodes, substrates were modified with acrylated silane to ensure covalent attachment of hydrogel structures to glass. We found that silanization of glass substrates containing unprotected Au patterns resulted in highly insulated and resistive electrodes. To resolve this problem, we did not remove the photoresist immediately after fabricating of the Au electrode arrays but used it as a protective layer during the silanization step. The photoresist layer was then removed after silane modification. Soluble ferricyanide redox species were used to test differences in electron transfer after silane modification of unprotected vs photoresist protected electrodes. As shown in cyclic voltammetry analysis presented in Figure 2B, the electrodes that were protected by photoresist during silanization were nearly as conductive as bare, unprocessed electrodes. In contrast, bare Au electrodes exposed to silane

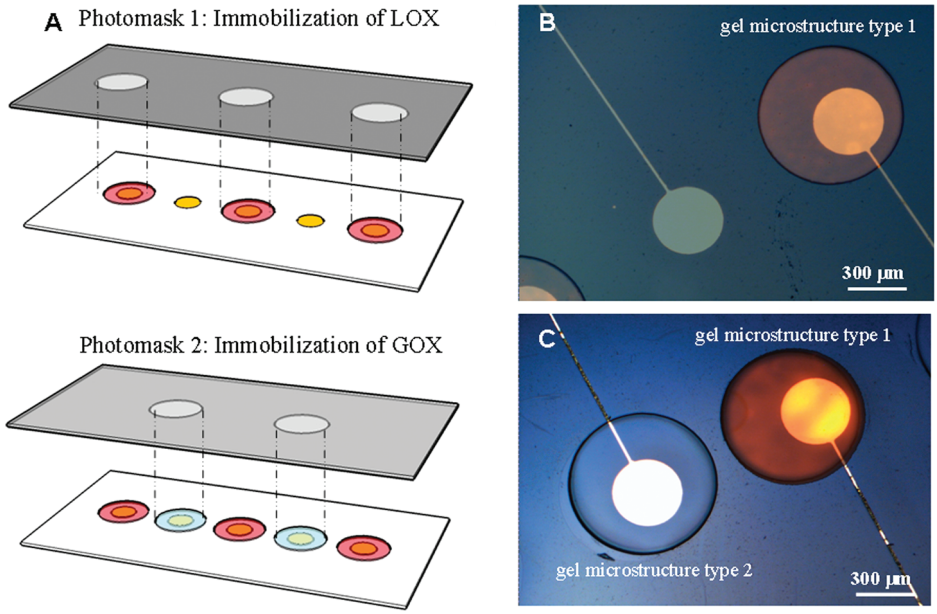

FIGURE 3. (A) Prepolymer formulations containing either GOX or LOX was spun onto the surface and exposed through a photomask. Subsequently, the second prepolymer formulation was spin-coated on the surface and registered with Au electrodes that remained unmodified. These sequential two mask process sequential two mask process resulted in fabrication of glucose- and lactate-sensitive electrodes in the same array. (B, C) Alignment and deposition of hydrogel microstructures of varying content on microfabricated Au electrodes. Hydrogel type 1 contains peroxidase/Amplex Red and becomes fluorescent when challenged with 5 mM H_2O_2, whereas hydrogel type 2 deposited on an adjacent electrode does not have these reporter molecules and remains insensitive to analyte.

solution were effectively insulated by the self-assembled organic layer and could not be used for electrochemistry experiments (Figure 2B).

Fabrication of Enzyme-Carrying Hydrogel Microstructures on Au Electrodes. Prior to enzyme immobilization, a layer of PEG hydrogel was micropatterned on the substrate so as to cover the leads while leaving open circular Au electrodes. This was necessary in order to decrease the background current and to enhance sensitivity of enzyme electrodes. As characterized by cyclic voltammetry with soluble ferricyanide (see Figure 2B), immobilizing pure PEG (not carrying redox species) on top of Au electrodes resulted in effective insulation of the electrodes. Combined with biocompatibility, insulating properties make PEG hydrogel an excellent bioelectrode packaging material.

As seen from Figures 1A and 2A, an electrode array represents a complex pattern comprising electrodes, leads, and contact pads. For array members to function as individual biosensors, enzymes must be placed exclusively onto specific electrodes without coating adjacent electrodes and/or interconnects. In this study, we employed PEG hydrogel photolithography method (29, 35) to deposit enzyme-carrying hydrogel microstructures onto desired members of an electrode array. Because PEG hydrogel patterning is analogous to traditional photoresist lithography, standard semiconductor tools, such as a mask aligner, could be employed to fabricate hydrogel microstructures in registration with microfabricated Au electrodes. Figure 2C shows two 300 μm diameter Au electrodes registered with 600 μm diameter PEG hydrogel elements.

Beyond depositing identical hydrogel microstructures on all electrodes, we wanted to highlight the possibility of placing hydrogel structures of distinct composition on adjacent electrodes. To help visualize this, we patterned two different PEG precursor solutions on Au electrodes using a two-mask process described diagrammatically in Figure 3A. The first PEG solution contained 50 μM Amplex Red and 0.1 mg/mL HRP, whereas the second precursor solution was pure PEG. Figure 3B shows Amplex Red/HRP containing hydrogel structure fabricated on top of one Au electrode, whereas the adjacent electrode remains bare. This image underscores our ability to spatially control placement of distinct hydrogel elements on a microfabricated surface. Exposure of this micropatterned surface to soluble 10 μM H_2O_2 initiated HRP-catalyzed breakdown of this molecule and conversion of nonfluorescent Amplex Red into a fluorescent intermediate resorufin (35). This resulted in coloration of the hydrogel structure seen in Figure 3C. In the next fabrication step, pure PEG precursor solution was photopolymerized adjacent to the enzyme-carrying hydrogel. When exposed to H_2O_2, HRP/Amplex Red-containing hydrogel element on the right changed color, whereas pure PEG element remained colorless (see Figure 3C). Images B and C in Figure 3 provide proof-of-concept demonstration that hydrogel microstructures of different composition can be fabricated on adjacent electrodes.

Characterizing Redox Activity of Hydrogel/Au Electrodes. After fabricating hybrid hydrogel/Au electrodes in a manner analogous to that described in Figure 3, we proceeded to characterize the response of these biosensors to analytes of interest: glucose and lactate. As discussed in the previous section, pure PEG hydrogel layer was found to be highly insulating, likely due to a small molecular weight PEG (MW 575) creating tight polymer mesh on top of an electrode. To improve conductivity, vinylferrocene was included into the prepolymer solution and became co-

valently incorporated into the PEG gel upon UV cross-linking. Incorporation of redox sites into the gel was also expected to mediate electron transfer from oxidoreductase enzymes to the electrode surface. This enzyme "wiring" strategy first described by Heller and colleagues (36) eliminates the reliance of glucose and lactate sensors on diffusible species such oxygen (co-substrate) and hydrogen peroxide (product). The oxygen tension and/or hydrogen peroxide concentration in the body or in the vicinity of cultured cells may vary and may contribute to erroneous sensor reading. Oxygen independence of glucose and lactate detection is described in the next section of this paper, whereas the redox activity of the gels is discussed below.

The activity of the redox species within the hydrogel was characterized by cyclic voltammetry at different scan rates ranging from 10 to 50 mV/s in PBS. As shown in Figure 4A, electrodes covered with redox hydrogels had anodic and cathodic peaks at 400 and 340 mV, respectively, which is consistent with redox behavior of ferrocene (37). The amplitude of anodic and cathodic peaks did not change appreciably when testing the electrodes after 2 weeks of incubation in PBS (data not shown), pointing to retention of the redox species in the gel. Importantly, Figure 4A also shows that peak splitting was unchanged as a function of scan rate, reverse-to-forward peak current ratio was close to unity and that the peak current increased proportionally to the scan rate (see Figure 4B). This suggests fast and reversible redox processes occurring in the PEG hydrogel-modified electrodes.

Importantly, electrodes within the same array worked independently. Figure 4C shows cyclic voltammograms from adjacent electrodes containing conductive hydrogel microstructures. As seen from these data, the current of two electrodes connected together was twice as high as that of individual electrodes. Similar testing was carried out before analyte detection to ensure that no short circuiting of the electrodes occurred after fabrication.

Detecting Glucose and Lactate with Enzyme-Carrying Hydrogel/Au Electrode Arrays. Amperometry was used to analyze the biosensor response to glucose and lactate of varying concentration. In these experiments, individual members of hydrogel/Au electrode array were poised at 0.4 V vs Ag/AgCl reference electrode and the changes in current in response to aliquotal addition of analyte were recorded. Figure 5A shows the current−time relationship of the hybrid hydrogel/electrode arrays to 2 mM glucose aliquots added into PBS solution (pH 7.0). As seen from these data, electrode response to glucose achieved saturation after 60 s; therefore, we chose this time interval between successive additions of glucose aliquots. The glucose calibration curve shown in Figure 5B was constructed by averaging the amperometric responses from a five-electrode array. The response was linear with an R^2 value of 0.99 and a sensitivity of 0.9 μA cm^{-2} mM^{-1} in the range from 0 to 20 mM. The standard deviation between members of the same electrode array was ~6%, whereas the standard deviation between devices was ~8% ($n = 5$). This underscores intra- and interdevice reproducibility of glucose response. The response of LOX-containing hydrogel/Au electrodes to lactate was characterized by amperometry in a manner similar to that described for glucose sensor above. Figure 5C,D shows the biosensor response to aliquotal addition of 1 mM lactate into PBS solution (pH 7) and the resultant calibration curve that was constructed by averaging response from a five-electrode array. The lactate response was linear with an R^2 value of 0.98 and a sensitivity of 1.1 μA cm^{-2} mM^{-1} in the range from 0 to 10 μM. The electrode responded rapidly to the addition of glucose and lactate, reaching 90% of the signal within 70 s.

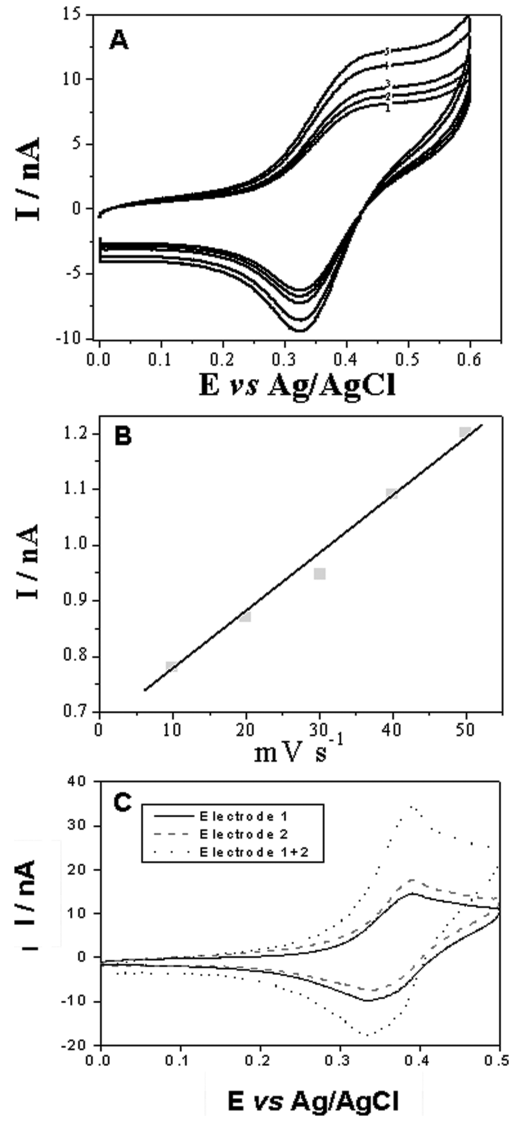

FIGURE 4. (A) Characterization of redox activity of vinylferrocene-containing hydrogel electrodes using cyclic voltammetry. Scan rate was varied from 10 to 100 mV/s. Ag/AgCl reference and Pt counter electrodes were used. (B) Linear relationship of anodic peak current vs scan rate suggests fast and reversible kinetics. (C) Demonstration that adjacent hydrogel electrodes were individually addressable. Comparison of redox activity of single hydrogel/Au electrode vs two electrodes connected together.

Although the sensitivity of the hydrogel-based electrodes described here is comparable to or better than some of the previous results reported by us and others (17, 22, 23, 38), there have been other studies demonstrating more sensitive

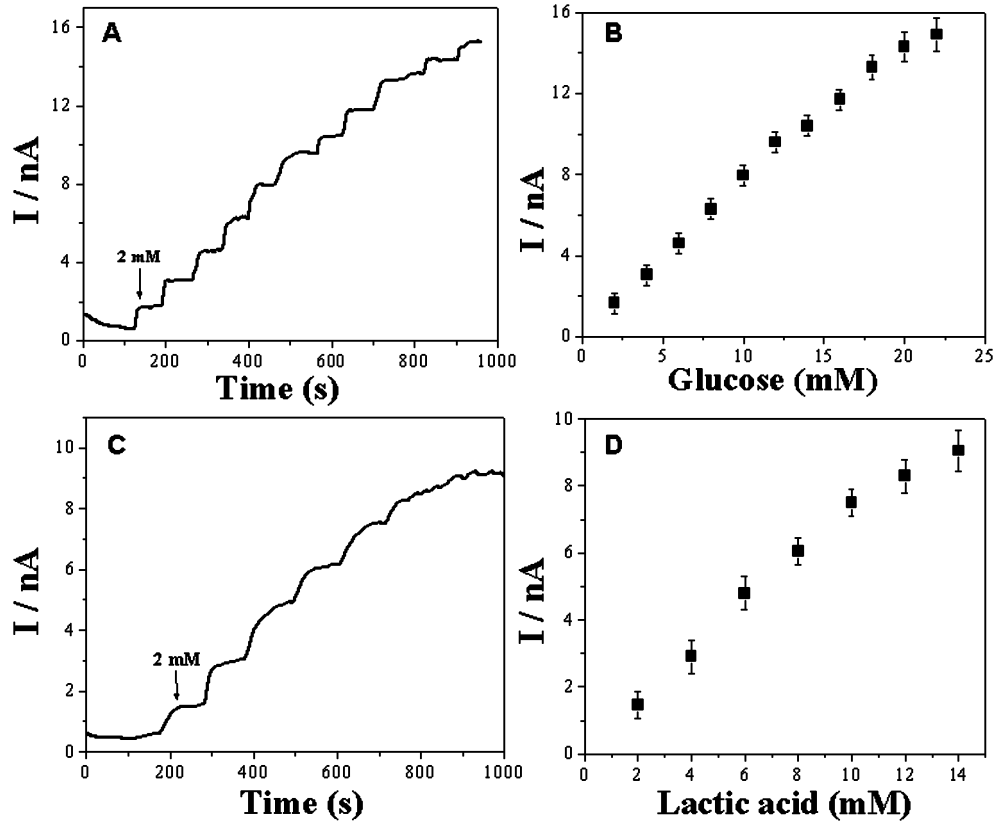

FIGURE 5. (A) Amperometric response of miniature enzyme electrodes to glucose. Microfabricated GOX-containing hydrogel/Au electrodes were poised at 0.4 mV vs Ag/AgCl reference electrode and were challenged with glucose in 2 mM increments. A current vs time response was recorded and averaged for five different devices ($n = 5$). (B) Calibration curve of GOX-based electrodes for 0 to 20 mM glucose range. (C) Amperometric response of LOX-containing hydrogel/Au electrodes to 2 mM aliquots of lactic acid. Conditions for testing the electrodes were identical to those discussed for glucose. (D) Calibration curve of lactate electrode showing response in the 0 to 10 mM range of analyte.

glucose electrodes (2, 39). In the future the sensitivity of our electrodes may be increased by altering gel composition.

The PEG photolithography afforded us the possibility to immobilize hydrogel structures of distinct composition onto members of the same electrode array (see Figure 3 for example). This strategy was used to construct electrode arrays where individual Au electrodes were functionalized with GOX- and LOX-carrying hydrogel microstructures. The ability of this biosensor array to detect two analytes, glucose and lactate, was then characterized by amperometry in a manner similar to that described for single analyte detection. Figure 6 demonstrates an experiment where adjacent electrodes containing GOX- and LOX-carrying hydrogels were connected together to a potentiostat and challenged first with lactic acid and then glucose. As seen from these data, the sensor first responded to lactate with sensitivity comparable to that demonstrated for a single lactate sensitive in Figure 5C. Subsequent exposure to glucose resulted in response equivalent to a single glucose sensitive electrode characterized in Figure 5A. These experiments demonstrate that both types of biosensors were present in the same electrode array.

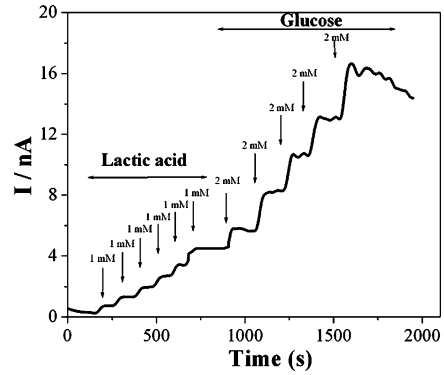

FIGURE 6. Connecting together two members of an electrode array, one GOX-containing hydrogel/Au electrode another LOX-carrying hydrogel/Au electrode. This electrode pair was challenged with lactic acid followed by glucose. Signals were recorder by amperometry by posing electrodes at 0.4 V vs Ag/AgCl reference. The response of an electrode pair to each analyte was comparable to that of individual glucose and lactate electrodes. This result shows that glucose and lactate can be detected in the same array of hydrogel/Au electrodes.

Stability and Oxygen Independence of Hydrogel-Based Enzyme Electrodes. It is very important that an enzyme-based biosensor is stable and is unaffected by changes in the surrounding environment. The stability of the biosensor was also investigated by challenging GOX-containing hydrogel/Au electrodes to 2 mM glucose daily for 15 days. As shown in Figure 7A glucose biosensor remained stable, retaining ~90% of its original response over this period of time.

Another important parameter tested was oxygen dependence of our biosensors. Oxygen is a cosubstrate consumed in the enzymatic breakdown of both glucose and lactate, and can be used for detection of both analytes. However, oxygen

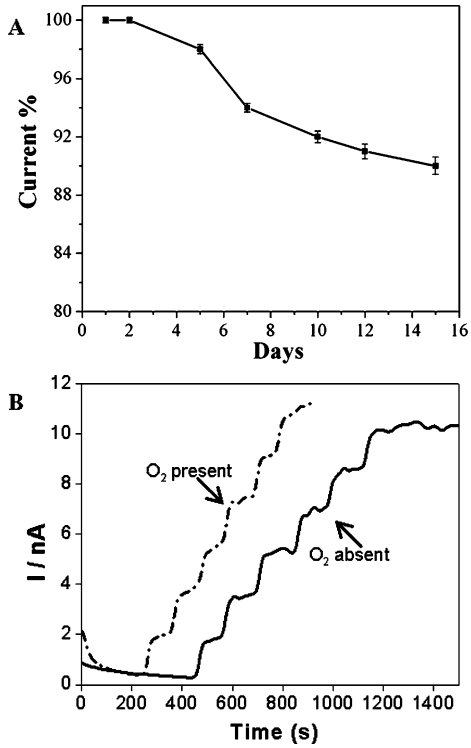

FIGURE 7. (A) Testing stability of glucose electrodes. Electrodes where stored at 4C in PBS and were tested daily by exposure to 6 mM glucose. Response to glucose was recorded as current vs time plot for five different devices ($n = 5$). (B) Response of GOX-carrying hydrogel/Au electrodes to 2 mM aliquots of glucose dissolved in oxygen-containing (21% oxygen) and oxygen-free PBS. Commercial oxygen electrode was used to verify oxygen tension of electrolyte solution. Electrode was poised at 0.4 V vs Ag/AgCl reference.

tension may vary in vivo or in proximity of metabolically active living cells in a culture dish. Heller and colleagues proposed to complex or "wire" enzymes to redox centers to enable direct electron transfer from the enzyme to the electrode via the redox sites, thus eliminating sensor dependence on oxygen (2, 36). In the present study, vinyl-terminated ferrocene was included into a prepolymer solution and became covalently incorporated into gel microstructures after photopatterning. As described in Figure 4 above, the redox sites were stably immobilized and electrochemically active within the hydrogel. To investigate the sensitivity of our biosensors to oxygen, we challenged GOX-containing hydrogel/Au electrodes with glucose dissolved in either PBS containing ambient oxygen (21%) or PBS solution that was deoxygenated by N_2 purging (0% oxygen as measured by commercial Clark-type electrode). Figure 6B shows signal from an enzyme electrode response to glucose dissolved in either oxygen-containing or oxygen-free electrolyte. A slightly lower (~8%) glucose signal was observed in the case of electrolyte containing oxygen. This difference in signal is minor; Heller et al. reported comparable differences in their "wired" electrodes (4). Although hydrogen peroxide oxidizes at much higher potentials (~0.7 V vs Ag/AgCl), minimal oxidation may be present in our experiments (performed at 0.4 V vs Ag/AgCl) and may contribute to a slightly higher signal in the presence of oxygen. This problem may be addressed in the future by selecting a redox molecule possessing lower formal potential.

CONCLUSIONS

Our paper describes the use of biomaterial microfabrication technique, PEG hydrogel photolithography, as a novel strategy for integrating miniature Au electrodes and enzyme-carrying hydrogel microstructures. PEG photolithography mimicked multilayer, multimask processes employed in semiconductor device fabrication and allowed us to immobilize GOX- and LOX-carrying hydrogels onto microfabricated Au electrode arrays. The biosensors were characterized electrochemically and exhibited a linear detection range of 20 mM for glucose and 10 mM for lactate. The sensitivity of the biosensors was 0.9 μA cm^{-2} mM^{-1} for glucose and 1.1 μA cm^{-2} mM^{-1} for lactate. Significantly, both glucose and lactate could be detected from the same electrode array. The microfabricated biosensors were highly reproducible with a standard deviation of 6% in glucose response between each array members and were stable after 2 weeks of testing. Inclusion of redox sites into the hydrogel ensured that enzyme electrodes were insensitive to oxygen tension. Besides providing an excellent matrix for enzyme entrapment, PEG hydrogels are nonfouling and have been used extensively by our group and others for micropatterning of living cells (40–43). In addition, we recently described sensing hydrogel microstructures that may be used to both sequester cells and to detect cell-secreted metabolites with fluorescence (32). The present paper provides a blueprint for fabricating and packaging miniature enzyme-based electrodes using a biocompatible, nonfouling, and cell-friendly polymer. In the future, dual functionality of PEG hydrogel microstructures as biosensors and cell culture chambers will be used for electrochemical detection of metabolite fluxes in the immediate vicinity of living cells.

Acknowledgment. The financial support for this study was provided by grants (NIH CA126716) and NSF (EFRI) awarded to AR. Additionally, A.L.S. acknowledges working at the National Science Foundation during the time this study was carried out. The views expressed in this article are those of the authors and do not reflect the views of the National Science Foundation.

REFERENCES AND NOTES

(1) Updike, S. J.; Hicks, G. P. *Nature* **1967**, *214*, 986–&.
(2) Pishko, M. V.; Michael, A. C.; Heller, A. *Anal. Chem.* **1991**, *63*, 2268–2272.
(3) Quinn, C. P.; Pishko, M. V.; Schmidtke, D. W.; Ishikawa, M.; Wagner, J. G.; Raskin, P.; Hubbell, J. A.; Heller, A. *Am. J. Physiol.* **1995**, *269*, E155.
(4) Ohara, T. J.; Rajagopalan, R.; Heller, A. *Anal. Chem.* **1994**, *66*, 2451–2457.
(5) Hu, Y.; Zhang, Y.; Wilson, G. S. *Anal. Chim. Acta* **1993**, *1993*, 503–511.
(6) O'Rahilly, S.; Vidal-Puig, A. *Science* **2001**, *431*, 125–126.
(7) Spiegelman, B. M.; Filer, J. S. *Cell* **2001**, *104*, 531–543.
(8) Gatenby, R. A.; Gillies, R. J. *Nat. Rev. Cancer* **2004**, *4*, 891–899.
(9) Jobst, G.; Moser, I.; Varahram, M.; Svasek, P.; Aschauer, E.; Trajanoski, Z.; Wach, P.; Kotanko, P.; Skrabal, F.; Urban, G. *Anal. Chem.* **1996**, *68*, 3173–3179.
(10) Moser, I.; Jobst, G.; Urban, G. *Biosens. Bioelectron.* **2002**, *17*, 297–302.

(11) Castillo, J.; Isik, S.; Blochl, A.; Pereira-Rodrigues, N.; Bedioui, F.; Csoregi, E.; Schuhmann, W.; Oni, J. *Biosens. Bioelectron.* **2005**, *20*, 1559–1565.
(12) Sato, N.; Okuma, H. *Anal. Chim. Acta* **2006**, *565*, 250–254.
(13) Urban, G. *Meas. Sci. Technol.* **2009**, *20*.
(14) Cohen, A.; Kunz, R. *Sens. Actuators, B* **2000**, *62*, 23–29.
(15) Lindner, E.; Cosofret, V. V.; Ulfer, S.; Johnson, T. A.; Ash, R. B.; Nagle, H. T.; Neuman, M. R.; Buck, R. P.; Fresenius, *J. Anal. Chem.* **1993**, *346*, 584–588.
(16) Koudelka-Hep, M.; Strike, D. J.; de Rooij, N. F. *Anal. Chim. Acta* **1993**, *281*, 461–466.
(17) Revzin, A.; Sirkar, K.; Simonian, A.; Pishko, M. V. *Sens. Actuators, B* **2002**, *81*, 359–368.
(18) Guenat, O. T.; Generelli, S.; de Rooij, N. F.; Koudelka-Hep, M.; Berthiaume, F.; Yarmush, M. L. *Anal. Chem.* **2006**, *78*, 7453–7460.
(19) Koudelka-Hep, M., De Rooij, N. F., Strike, D. J. In *Immobilization of Enzymes and Cells*; Guisan, J. M., Ed.; Methods in Biotechnology; Humana Press: Totowa, NJ, 1997; Vol. 1, pp 83—85.
(20) Malitesta, C.; Palmisano, F.; Torsi, L.; Zambonin, P. G. *Anal. Chem.* **1990**, *62*, 2735–2740.
(21) Strike, D. J.; De Rooij, N. F.; Koudelka-Hep, M. In Immobilization of Enzymes and Cells; Guisan, J. M., Ed.; Methods in Biotechnology; Humana Press: Totowa, NJ, 1997; Vol. 1, pp 93—100.
(22) Sirkar, K.; Revzin, A.; Pishko, M. V. *Anal. Chem.* **2000**, *72*, 2930–2936.
(23) Wang, Y. D.; Joshi, P. P.; Hobbs, K. L.; Johnson, M. B.; Schmidtke, D. W. *Langmuir* **2006**, *22*, 9776–9783.
(24) Jimenez, C.; Bartrol, J.; deRooij, N. F.; KoudelkaHep, M. *Anal. Chim. Acta* **1997**, *351*, 169–176.
(25) Belmont-Hebert, C.; Tercier, M. L.; Buffle, J.; Fiaccabrino, G. C.; de Rooij, N. F.; Koudelka-Hep, M. *Anal. Chem.* **1998**, *70*, 2949–2956.
(26) Mugweru, A.; Clark, B. L.; Pishko, M. V. *Electroanalysis* **2007**, *19*, 453–458.
(27) Takatsu, I.; Moriizumi, T. *Sens. Actuators* **1987**, *11*, 309–317.
(28) Jimenez, C.; Bartroli, J.; Derooij, N. F.; Koudelkahep, M. *Sens. Actuators, B* **1995**, *27*, 421–424.
(29) Revzin, A.; Russell, R. J.; Yadavalli, V. K.; Koh, W.-G.; Deister, C.; Hile, D. D.; Mellott, M. B.; Pishko, M. V. *Langmuir* **2001**, *17*, 5440–5447.
(30) Wagner, J. G.; Schmidtke, D. W.; Quinn, C. P.; Fleming, T. F.; Bernacky, B.; Heller, A. *Proc. Natl. Acad. Sci. U.S.A.* **1998**, *95*, 6379–6382.
(31) Russell, R. J.; Pishko, M. V.; Simonian, A. L.; Wild, J. R. *Anal. Chem.* **1999**, *71*, 4909–4912.
(32) Yan, J.; Sun, Y. H.; Zhu, H.; Marcu, L.; Revzin, A. *Biosens. Bioelectron.* **2009**, *24*, 2604–2610.
(33) Koh, W. G.; Pishko, M. *Sens. Actuators, B* **2005**, *106*, 335–342.
(34) Zhu, H.; Yan, J.; Revzin, A. *Colloids Surf., B* **2008**, *64*, 260–268.
(35) Zhou, M.; Diwu, Z.; Panchuk-Voloshina, N.; Haugland, R. P. *Anal. Biochem.* **1997**, *253*, 162–168.
(36) Degani, Y.; Heller, A. *J. Am. Chem. Soc.* **1989**, *111*, 2357–2358.
(37) Ju, H.; Leech, D. *J. Chem. Soc., Faraday Trans.* **1997**, *93*, 1371–1375.
(38) Hodak, J.; Etchenique, R.; Calvo, E. J.; Singhal, K.; Bartlett, P. N. *Langmuir* **1997**, *13*, 2708–2716.
(39) Merchant, S. A.; Tran, T. O.; Meredith, M. T.; Cline, T. C.; Glatzhofer, D. T.; Schmidtke, D. W. *Langmuir* **2009**, *25*, 7736–7742.
(40) Revzin, A.; Tompkins, R. G.; Toner, M. *Langmuir* **2003**, *19*, 9855–9862.
(41) Suh, K. Y.; Seong, J.; Khademhosseini, A.; Laibinis, P. E.; Langer, R. *Biomaterials* **2004**, *25*, 557–563.
(42) Lee, J. Y.; Shah, S. S.; Yan, J.; Howland, M. C.; Parikh, A. N.; Pan, T. R.; Revzin, A. *Langmuir* **2009**, *25*, 3880–3886.
(43) Zhu, H.; Stybayeva, G. S.; Silangcruz, J.; Yan, J.; Ramanculov, E.; Dandekar, S.; George, M. D.; Revzin, A. *Anal. Chem.* **2009**, *81*, 8150–8156.

AM9007819